$KEr(MoO_4)_2$: A quasi-one-dimensional $S=\frac{3}{2}$ Blume-Capel system

D. Horváth*
Department of Theoretical Physics and Geophysics, P.J. Šafárik University, Moyzesova 16, 041 54 Košice, Slovakia

A. Orendáčová and M. Orendáč
Department of Experimental Physics, P. J. Šafárik University, Park Angelinum 9, 041 54 Košice, Slovakia

M. Jaščur
Department of Theoretical Physics and Geophysics, P. J. Šafárik University, Moyzesova 16, 041 54 Košice, Slovakia

B. Brutovský
Department of Biophysics, P. J. Šafárik University, Jesenná 5, 041 54 Košice, Slovakia

A. Feher
Department of Experimental Physics, P. J. Šafárik University, Park Angelinum 9, 041 54 Košice, Slovakia
(Received 20 November 1998; revised manuscript received 8 February 1999)

In this paper we present experimental data and Monte Carlo calculations of $KEr(MoO_4)_2$ specific heat in the temperature range 0.4–6 K and in magnetic field B from 0–1 T applied along the easy axis. The data analysis for $B=0$ has identified $KEr(MoO_4)_2$ as an $S=3/2$ Blume-Capel model on rectangular lattice with the intrachain exchange interaction $\tilde{J}_1/k_B=0.38$ K, interchain exchange interaction $\tilde{J}_2/k_B=-0.07$ K, and single-ion anisotropy $D/k_B=10$ K, with the ordering temperature $T_c=0.95$ K. Further Monte Carlo studies of the Blume-Capel model in the magnetic field applied along the easy axis have been focused on the formation of cluster excitations in a paramagnetic regime. The magnetic-field dependence of a cluster mean length studied in the chain direction exactly follows the behavior of $S=1/2$ Ising chain at least for the given set of $\tilde{J}_1$, $\tilde{J}_2$, and D parameters. On the other hand, the specific heat in nonzero field represents a more sensitive quantity to the presence of interchain correlations and the occupation of a higher doublet. [S0163-1829(99)11025-7]

I. INTRODUCTION

The study of magnetic excitations in one-dimensional magnetic systems has been a subject of intensive theoretical and experimental studies for a few decades.[1,2] The spin dynamics of $S=1/2$ Heisenberg-Ising linear ferromagnet described by the Hamiltonian

$$\mathcal{H}^{\mathrm{HI}}=-2J\sum_i\left[S_i^zS_{i+1}^z-\frac{1}{4}+\gamma(S_i^xS_{i+1}^x+S_i^yS_{i+1}^y)\right], \tag{1}$$

where γ is an anisotropy parameter which varies between the Ising model ($\gamma=0$) and isotropic Heisenberg model ($\gamma=1$), was theoretically investigated by Johnson and Bonner.[3] The zero-field studies have revealed that for $0.6\leqslant\gamma\leqslant1$ the spin waves are dominating excitations from the ground state (spin-wave regime) while for $0\leqslant\gamma<0.6$ the dominant excitations are bound complexes of neighboring spins easily visualizable in the Ising limit (bound magnon regime). Spin clusters—the spin excitations from the ground state of the Hamiltonian (1) in a longitudinal field (applied along the easy axis z)—were theoretically studied in detail for $\gamma=0$ in Ref. 4. In the same work the theory was applied to the interpretation of electron spin-resonance data obtained on exchange-coupled quasi-one-dimensional Ising ferromagnet $CoCl_2\cdot2H_2O$. The contribution of the spin cluster excitations to the specific heat of $KEr(MoO_4)_2$ previously identified as a quasi-one-dimensional $S=1/2$ Ising ferromagnet,[5] was studied in Ref. 6. The analysis revealed a significantly different behavior of data in low magnetic fields. The deviations from the theoretical predictions were ascribed to the influence of interchain coupling and a presence of transverse spin components. $KEr(MoO_4)_2$ belongs to the series of rare-earth compounds with a general formula $XR(Mo_4)_2$ ($X=Cs,K,Rb,\ldots,R=La,Ce,\ldots,Lu$) representing systems with a layered crystal structure. In these ionic crystals the R^{3+} ions occupy sites which are sufficiently far apart from one another so that dipolar coupling represents the dominating interaction among magnetic moments.[7] The ground state of a free Er^{3+} is $^4I_{15/2}$. In the $KEr(MoO_4)_2$ lattice the $2J+1$ degeneracy of the electronic state is removed by the perturbing effects of the local crystalline field (CEF) of symmetry C_2 and is split into eight Kramers doublets with the lowest energies $E_0=0$, $E_1=13\ \mathrm{cm}^{-1}$, and $E_2=32\ \mathrm{cm}^{-1}$.[8] The Ising character of this compound is quite well established by a strong g-factor anisotropy with

$$g_a=1.8,\quad g_b<0.9,\quad \text{and}\quad g_c=14.7 \tag{2}$$

for the lowest doublet. The energy of the first excited doublet was re-estimated as $E_1=15\pm2\ \mathrm{cm}^{-1}$ with corresponding g factors[9]

$$g_{a'}=2.3,\quad g_{b'},g_{c'}<1. \tag{3}$$

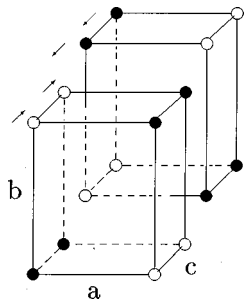

FIG. 1. Ground-state configuration of $KEr(MoO_4)_2$ magnetic structure calculated in a pure dipolar approach (open and solid circles correspond to opposite directions of the moments).

Theoretical calculations considering only dipolar interactions and CEF effects have shown that the magnetic structure of the ground state consists of dipolar ferromagnetic chains parallel to the *c* axis with magnetic moments oriented along the chains. The moments in neighboring chains are coupled antiferromagnetically[9] (Fig. 1). Similar dipolar calculations performed for $CsDy(MoO_4)_2$ resulted in the qualitatively same ground-state configuration[10] which was recently confirmed by elastic neutron-scattering experiments performed on $CsDy(MoO_4)_2$ single crystal at 0.5 K, i.e., in the ordered state.[11]

On the basis of the aforementioned facts the title compound might be an interesting subject of resonance and thermodynamic studies of nonlinear magnetic excitations (spin-cluster excitations) in Ising system with long-range interactions. However, in spite of the recent progress in the study of Ising systems, there is still lack of theories including long-range interactions. Thus in the first step we have analyzed the relevant system within exchange-coupled models characterized by short-range interactions. In particular, the present work is devoted to the theoretical and experimental study of $KEr(MoO_4)_2$ specific heat. The analysis of data has been performed within spin-3/2 Blume-Capel (BC) model on the rectangular lattice. In general, the exact solution for the spin-3/2 BC model is not known even in the case of planar lattices,[12] although recently some special cases have been solved exactly.[13] These solutions, however, do not include any case with the external field. For that reason we have applied the standard single-spin-flip Monte Carlo (MC) algorithm[14,15] to focus our attention on the study of spin cluster excitations in the longitudinal field and their contribution to the specific heat of the studied system.

The outline of this paper is as follows. Section II is devoted to the analysis of a temperature dependence of $KEr(MoO_4)_2$ specific heat in the zero magnetic field. In this section the $S=3/2$ BC model on the rectangular lattice is introduced. In addition, further statistical quantities are defined to extend our understanding of the processes on the microscopic level. The magnetic field dependence of $KEr(MoO_4)_2$ specific heat in a magnetic field applied along the easy axis is discussed in Sec. III. The main conclusions are summarized in the Sec. IV.

II. MODEL OF $KEr(MoO_4)_2$ IN ZERO EXTERNAL MAGNETIC FIELD

A. Model of $KEr(MoO_4)_2$

Previous specific-heat studies carried out from 0.4–6 K in zero magnetic field have indicated assumed low-dimensional

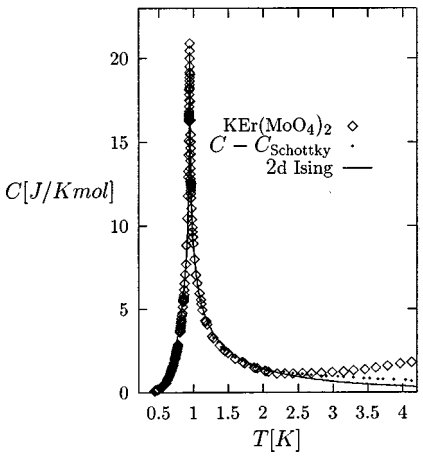

FIG. 2. Specific heat of a single crystal of $KEr(MoO_4)_2$ versus temperature (◇); the resultant $KEr(MoO_4)_2$ specific heat obtained by subtraction of the contribution of crystal-field levels is represented by dots; the solid line represents exact specific-heat results numerically calculated for $|J_1|/k_B=0.85$ K, $|J_2/J_1|=0.19$. (For clarity, the specific heat data from the nearest surrounding of the phase transition, exceeding the value of 25 J/K mol, are not shown).

behavior of the magnetic system.[5] The compound was identified as a quasi-two-dimensional array of coupled $S=1/2$ Ising chains with intrachain interaction $|J_1|/k_B \approx 0.9$–1.4 K and interchain interaction $0.01J_1 < |J_2| < 0.1J_1$. This relatively large dispersion in J_1, J_2 values might result from the analysis performed on the basis of the approximate effective-field theory for $S=1/2$ rectangular Ising lattice. Since this approach does not yield accurate results in the vicinity of the phase transition observed at $T_c=0.95$ K, to avoid the inaccuracies involved by the approximation, the exact Onsager's solution of this model[16] was applied yielding $|J_1|/k_B=0.85$ K and $|J_2/J_1| \approx 0.2$. Despite the good description of experimental data near the phase transition, the disagreement between the data and exact theory still persists at temperatures above 2 K, with rising differences towards higher temperatures; e.g., at the temperature 4 K the difference between the data and theoretical prediction takes about 50% (Fig. 2). These deviations might be ascribed to the direct subtraction of the contribution of a higher doublet with the energy $E_1 = 15\ \mathrm{cm}^{-1}$.

To verify this assumption in detail, a more complex model was suggested for $KEr(MoO_4)_2$; since in the aforementioned temperature range only the two lowest doublets govern the thermodynamics of our system, the system can be treated as an $S'=3/2$ rectangular Ising lattice with

$$D=(E_1-E_0)/2, \tag{4}$$

which represents the realization of $S=3/2$ BC model[17,18] on a rectangular lattice given by the Hamiltonian

$$\mathcal{H}^{\mathrm{BC}} = -\tilde{J}_1 \sum_{i,j} S^z_{i,j} S^z_{i+1,j} - \tilde{J}_2 \sum_{i,j} S^z_{i,j} S^z_{i,j+1} + \sum_{i,j} \mathcal{H}_0(S^z_{i,j}), \tag{5}$$

$$\mathcal{H}_0(S^z) = D\left[\frac{9}{4} - (S^z)^2\right], \quad S^z = \pm\frac{3}{2}, \pm\frac{1}{2}, \tag{6}$$

where $S^z_{i,j}$ is the spin projection at the site position i,j, $\mathcal{H}_0(S^z)$ is the single-site part of the Hamiltonian [we used the calibration $\mathcal{H}_0(3/2)=E_0$, $\mathcal{H}_0(1/2)=E_1$]; $\tilde{J}_1$ ($\geqslant 0$), $\tilde{J}_2$ ($\leqslant 0$), represent the intrachain, interchain nearest-neighbor interactions, respectively, and D stands for the single-ion anisotropy parameter. We should note that the $\tilde{J}_1$, $\tilde{J}_2$ signs were chosen to mimic the dipolar nature of the interactions despite the specific heat is not sensitive to the sign of the interaction.

B. Calculation techniques

The model (5) is not exactly soluble, thus the MC method was used to provide the theoretical predictions of a sufficient accuracy. Since the MC calculations require much computational time, the MC method is not an effective tool for fitting the experimental data to determine the values of $\tilde{J}_1,\tilde{J}_2$ and D parameters. However, the important fact useful for finding $\tilde{J}_1,\tilde{J}_2$ values is that D of the studied system is quite large with respect to the temperatures of our interest, more precisely $\max(T,T_c)\ll 2D/k_B$ and $D\gg\max(|\tilde{J}_1|,|\tilde{J}_2|)$. The latter guarantees the dominance of $S^z=\pm 3/2$ projections and the equivalence of $D(S^z)^2$ and $9D/4$ terms. The appropriate rescaling of the spin variable $S^z=(3/2)\sigma^z$ ($\sigma^z=\pm 1$) in $\mathcal{H}^{BC}$ demonstrates a direct correspondence between BC and Ising model

$$\mathcal{H}^I=\mathcal{H}^{BC}\big|_{S^z=(3/2)\sigma^z}=-J_1\sum_{i,j}\sigma^z_{i,j}\sigma^z_{i+1,j}-J_2\sum_{i,j}\sigma^z_{i,j}\sigma^z_{i,j+1}, \tag{7}$$

where $\tilde{J}_1=(4/9)J_1$ and $\tilde{J}_2=(4/9)J_2$. Owing to this fact, we used the previous estimates of J_1,J_2 to determine

$$\tilde{J}_1/k_B=0.38\ \text{K},\quad \tilde{J}_2/k_B=-0.07\ \text{K}. \tag{8}$$

The value $D/k_B=10.8$ K was estimated from electron paramagnetic resonance (EPR) experiment[9] using Eq. (4).

The physical quantity of the main interest is the specific heat which can be calculated by using the fluctuation-dissipation formula

$$C=R\frac{\langle E^2\rangle-\langle E\rangle^2}{(k_BT)^2L^2}. \tag{9}$$

Here $\langle\ldots\rangle$ means the ensemble average and $\langle E\rangle$ is the mean energy of a lattice involving L^2 spins, $R=k_BN_A$ is the gas constant (N_A is Avogadro's number).

Considerable information about the anisotropy of a system is provided by the nearest-neighbor values $\langle\mathcal{G}_1\rangle$ and $\langle\mathcal{G}_2\rangle$ of intrachain and interchain static pair-correlation functions. The values have been obtained by averaging of $\mathcal{G}_1$ and $\mathcal{G}_2$:

$$\mathcal{G}_1=\frac{1}{(L-1)L}\sum_{i=1}^{L-1}\sum_{j=1}^{L}S^z_{i,j}S^z_{i+1,j},$$

$$\mathcal{G}_2=\frac{1}{(L-1)L}\sum_{i=1}^{L}\sum_{j=1}^{L-1}S^z_{i,j}S^z_{i,j+1}. \tag{10}$$

To simplify the description of the clustering of the two-dimensional system, we focused our attention on the formation of clusters in the chain direction parallel to the c axis. Thus the notion of the spin ferromagnetic chains of the length $l_1^{(0)}$ was introduced as the sequence

$$\{S^z_{i,j},S^z_{i+1,j},\ldots,S^z_{i+l_1^{(0)}-1,j},S^z_{i+l_1^{(0)},j}\} \tag{11}$$

picked out from MC snapshot to satisfy the properties

$$S^z_{i,j}=S^z_{i+1,j}=\ldots=S^z_{i+\ell_1^{(0)}-1,j}=S^z_{i+\ell_1^{(0)},j},$$
$$\underbrace{S^z_{i-1,j}\neq S^z_{i,j}}_{\text{pair break}},\qquad \underbrace{S^z_{i+\ell_1^{(0)},j}\neq S^z_{i+\ell_1^{(0)}+1,j}}_{\text{pair break}}. \tag{12}$$

A statistical quantity associated to $l_1^{(0)}$ is the mean length of the ferromagnetic chains $\langle l_1^{(0)}\rangle$ ($1\leqslant\langle l_1^{(0)}\rangle\leqslant L$), which can be calculated via the expression

$$\langle l_1^{(0)}\rangle=\left\langle\frac{L}{1+(L-1)\rho_b}\right\rangle, \tag{13}$$

where density of the boundary pair breaks ρ_b is defined by

$$\rho_b=1-\frac{1}{(L-1)L}\sum_{i=1}^{L-1}\sum_{j=1}^{L}\delta_{S^z_{i,j},S^z_{i+1,j}},\quad 0\leqslant\rho_b\leqslant 1. \tag{14}$$

(Here the used Kronecker symbol δ is generalized for the fractional indices.)

To describe the relative occupation of $\pm 3/2$ and $\pm 1/2$ doublets, we introduced the probability

$$p(S^z)=\text{Prob}(S^z_{ij}=S^z)=\langle\delta_{S^z_{ij},S^z}\rangle \tag{15}$$

satisfying the normalization condition $p(-1/2)+p(-3/2)+p(3/2)+p(1/2)=1$.

The MC simulations of the equilibrium temperature dependences were performed by starting at 5 K from a randomly chosen spin configuration (close to the expected paramagnetic state). Then the spin system was cooled with the temperature step $\Delta T\simeq 0.1$ K down to 0.4 K. After each step ΔT, 5×10^4 MC steps/spin were carried out to equilibrate the system. Consequently, 3×10^5 MC steps/spin were done to calculate the statistical averages of interest. The simulations were performed for the $\tilde{J}_1,\tilde{J}_2$ given by Eq. (8) and $D/k_B=10.8$ K revealing the fact that the system size $L=30$ is sufficient to guarantee that the contribution of the finite-size effects does not exceed the nominal 5% inaccuracy of the experimental data[5] except the critical region (Fig. 3) which is well described by the Onsager's solution for the model (7).

C. Analysis of the MC results

The treatment of the MC data indicates the spontaneous transition from the paramagnetic to antiferromagnetically ordered phase at the temperatures approaching the value of the pseudocritical temperature $T_c(L)$. It was found that $T_c(30)=0.96\pm 0.01$ K estimated from the peak of $C(T)$ coincides with the experimentally observed $T_c=0.955\pm 0.005$ K.

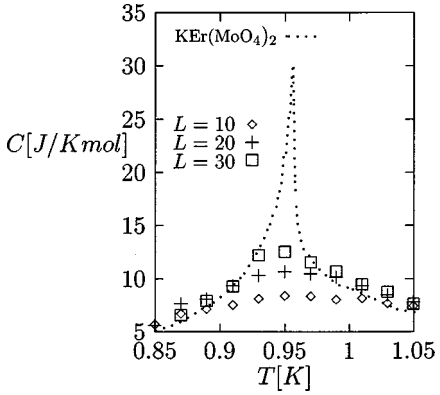

FIG. 3. Temperature dependence of $KEr(MoO_4)_2$ specific heat near the critical point (dots) and the MC simulations for $L=10$, 20, and 30 with $\tilde{J}_1$ and $\tilde{J}_2$ given by Eq. (8) and $D/k_B=10.8$ K.

The results of the MC simulations for the given set of $\tilde{J}_1,\tilde{J}_2$ and D parameters are drawn in Fig. 4. For $T<2$ K the specific heat of BC model coincides with the Onsager's solution of Eq. (7). A slight but systematic discrepancy between the MC results and data observed at higher temperatures, taking about 20% at 4 K, might persist due to approximative separation of the lattice contribution and/or

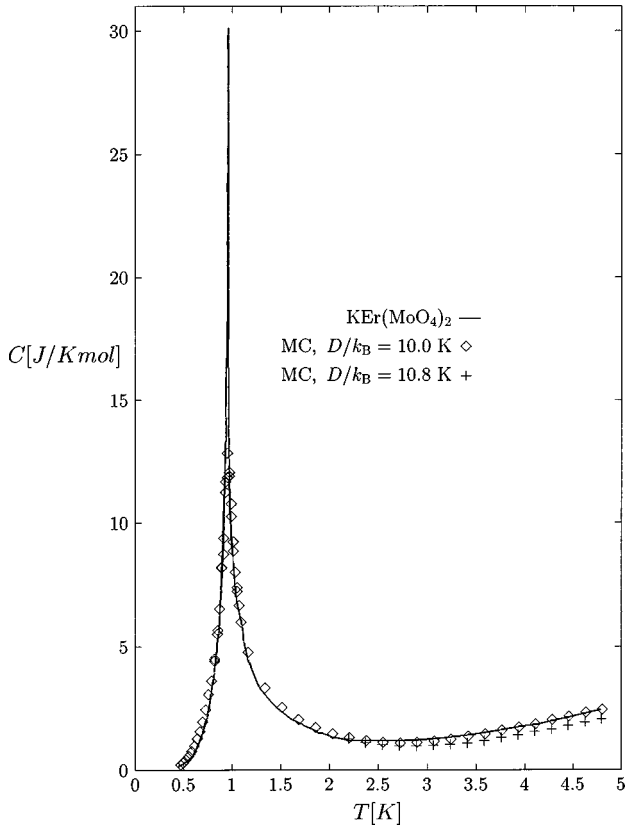

FIG. 4. Temperature dependence of $KEr(MoO_4)_2$ specific heat with only lattice contribution subtracted (solid line) and MC results obtained for the Hamiltonian (5) and (6) with the parameters $\tilde{J}_1/k_B=0.38$ K, $\tilde{J}_2/k_B=-0.07$ K, and $D/k_B=10.8$ K (+) and with the parameters $\tilde{J}_1/k_B=0.38$ K, $\tilde{J}_2/k_B=-0.07$ K, and $D/k_B=10.0$ K ($\diamond$) calculated for the lattice size $L=30$.

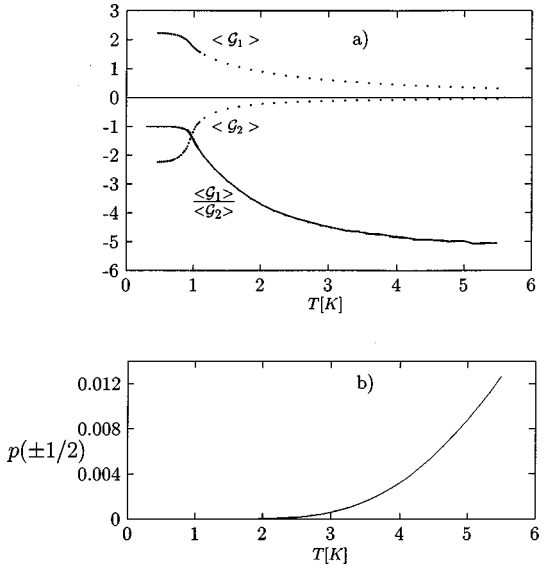

FIG. 5. (a) The temperature dependence of $\langle\mathcal{G}_1\rangle,\langle\mathcal{G}_2\rangle$ and their ratio $\langle\mathcal{G}_1\rangle/\langle\mathcal{G}_2\rangle$ calculated using MC sampling for $L=30$ and parameters $\tilde{J}_1/k_B=0.38$ K, $\tilde{J}_2/k_B=-0.07$ K, and $D/k_B=10.0$ K. (b) The temperature dependence of the occupation probability of a higher doublet $p(\pm 1/2)$ calculated for the same parameters as in Fig. 5(a).

experimental inaccuracy of D, so further MC trials were concentrated on the finding of a more appropriate D value. They revealed the alternative value

$$D/k_B=10\,\mathrm{K}, \tag{16}$$

which provides a good agreement between the theory and experiment (Fig. 4). It should be noted that the difference between the original and alternative estimation of D value still lies within the experimental inaccuracy of EPR estimation. Further conjecture stemming from MC studies is illustrated in Fig. 5(a). It shows the temperature dependence of the ratio $\langle\mathcal{G}_1\rangle/\langle\mathcal{G}_2\rangle$. This ratio is the measure of the competition of the intrachain and interchain coupling effects; while for $T<T_c$ the strength of both kinds of spin correlations is comparable, the anisotropy of spin-spin correlations for $T>T_c$ indicates the decoupling of the planar system into chains. The MC calculation of the probability of the occupation of the higher doublet $p(\pm 1/2)$ [Fig. 5(b)] demonstrates that under 2 K the studied system coincides with the model (7). Thus, on the basis of these facts, in the temperature region $2<T<3$ K the system behavior may be approximated by $S=1/2$ Ising chain. This simplification represents an intermediate step for understanding of the spin-cluster excitations in the magnetic field applied along the easy axis.[4,19]

III. SPECIFIC HEAT OF $KEr(MoO_4)_2$ IN EXTERNAL MAGNETIC FIELD PARALLEL TO THE EASY AXIS

A. The modification of the model for $B\neq 0$

Specific heat of the single-crystal $KEr(MoO_4)_2$ of weight of 1 g was measured in the temperature range from 2–6 K by using a standard adiabatic calorimetry in the fields up to 1 T applied along the crystallographic c axis which was declared by the previous studies to be the easy axis of the magnetic

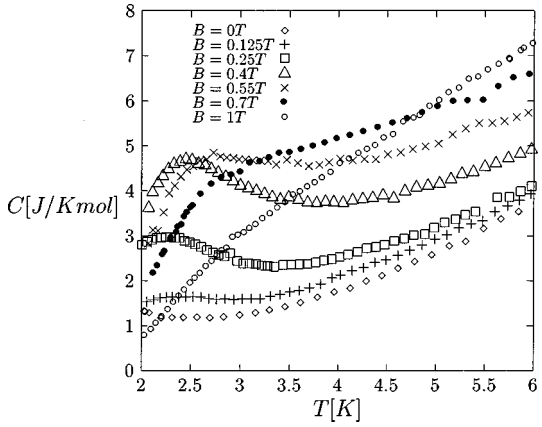

FIG. 6. Temperature dependence of the single crystal KEr$(MoO_4)_2$ specific heat in zero magnetic field ($\diamond$) and fields $B\|c$; $B=0.125$ T (+),0.25 T (□), 0.4 T (△), 0.55 T(×), 0.7 T (●),1 T (○) (lattice contribution subtracted).

system (Fig. 6). The inacuracy of the data did not exceed 3%. Experimental details are described elsewhere.[20] A lattice contribution was subtracted from the experimental data using the method described in Ref. 5. As was shown above, zero magnetic-field MC calculations suggest to treat the system as an $S=1/2$ Ising ferromagnetic chain in the narrow temperature range from 2–3 K—the result of a compromise between the strength of decoupling of the system into chains and the occupation of the higher doublet. Thus the temperature dependences of the specific heat in Fig. 6 cannot be analyzed within one-dimensional (1D) $S=1/2$ model in the whole temperature region and further analysis was performed at two chosen temperatures: $T_1=2.5$ K and $T_2=4.27$ K. The former should represent a more regular condition for applying the $S=1/2$ theory of spin-cluster excitations[4,19] to the data analysis. Thus using the current data the magnetic-field dependence of the specific heat at a constant temperature was obtained (Figs. 7 and 8), however, the low number of experimental data does not allow us to make a detailed quantitative analysis. The comparison of the experimental data with the theoretical prediction for $S=1/2$ Ising chain in the magnetic

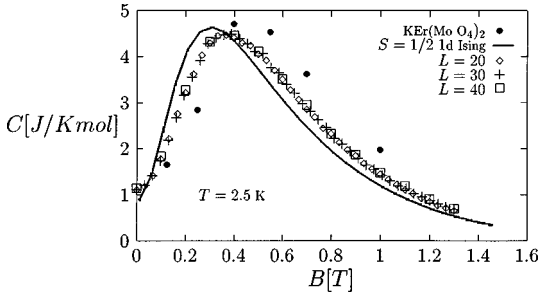

FIG. 7. Specific heat of the single crystal KEr$(MoO_4)_2$ versus magnetic field $B\|z$ at the temperature $T_1=2.5$ K (●). The solid line represents $S=1/2$ Ising ferromagnetic chain with $J_1/k_B=0.85$ K plotted simultaneously with the MC results for $S=3/2$ BC model with $\tilde{J}_1/k_B=0.38$ K,$\tilde{J}_2/k_B=-0.07$ K, and $D/k_B=10$ K calculated on the lattice size $L=20$, 30, and 40. The comparison of the data for different system sizes shows that finite-size effects are not essential with respect to the difference between the MC and experimental results.

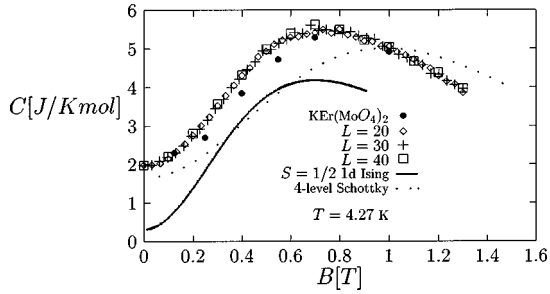

FIG. 8. Specific heat of the single crystal KEr$(MoO_4)_2$ versus magnetic field $B\|z$ at the temperature $T_2=4.27$ K (●). The solid line represents $S=1/2$ Ising ferromagnetic chain with $J_1/k_B=0.85$ K. The results of the MC calculations for $S=3/2$ BC model with $\tilde{J}_1/k_B=0.38$ K,$\tilde{J}_2/k_B=-0.07$ K and $D/k_B=10$ K were obtained for $L=20$, 30, and 40. The Schottky contribution of the two lowest Kramers doublets separated by the energy $2D/k_B=20$ K split in a magnetic field is represented by a dotted line.

field applied along the easy axis[19] is shown in Figs. 7 and 8. As can be seen, at the temperature T_1 the behavior of the system may be roughly approximated by the specific-heat contribution of spin-cluster excitations theoretically predicted in $S=1/2$ Ising ferromagnetic chain in the magnetic field parallel to the easy axis[4] resulting in a single round maximum. Observation of the round maximum represents a strong indication of the ferromagnetic nature of intrachain interaction since, as was predicted in Ref. 19, the intrachain antiferromagnetic interaction gives rise to a double peak structure of the specific heat versus magnetic-field dependence. Previous zero-field analysis was not able to determine the character of the interactions due to the fact that the specific heat of Ising system in zero magnetic field is not sensitive to the sign of interaction. Furthermore, recent specific-heat studies of H_c-T_c phase diagram[21] point to the antiferromagnetic character of the interchain coupling. Thus in a rough approximation we could note that the signs of the interactions correspond to those theoretically predicted within the pure dipolar approach,[9] namely, $\tilde{J}_1>0$, $\tilde{J}_2<0$. The combined effect of the crystal and external magnetic field $B\|z$ can be incorporated into a generalized single-site part of BC Hamiltonian (6):

$$\mathcal{H}_0(S^z)=D\left[\frac{9}{4}-(S^z)^2\right]-\frac{1}{2}g(|S^z|)\,\mu_B\,\mathrm{sgn}(S^z)\,B, \tag{17}$$

$$g(x)=\begin{cases} g_c, & x=3/2, \\ g_{c'}, & x=1/2. \end{cases} \tag{18}$$

By using Eqs. (5) and (17) we can easily verify that the application of a magnetic field of a supercritical value,

$$B>B_c=\frac{9|\tilde{J}_2|}{2\,g_c\,\mu_B}, \quad (B_c\simeq 32\ \text{mT}), \tag{19}$$

changes the antiferromagnetic ground state,

$$S^z_{i,j}=S^z_{i+1,j}=-S^z_{i,j+1}=\frac{3}{2}\,\mathrm{sgn}\,(S^z_{i,j}),\quad \forall(i,j),\quad B<B_c, \tag{20}$$

and leads to the ferromagnetic state consisting of the pure $S^z_{i,j}=3/2$ projections. Consequently, for $B>B_c$, any spin flips $S^z_{i,j}\neq 3/2$ can be considered as spin excitations. The formation of two-dimensional clusters of the excitations studied in the chain direction can be quantified by mean length $\langle l_1^{(B)}\rangle$ in analogy with Eq. (13). Now the chain clusters $\{S^z_{i,j}, S^z_{i+1,j}, \ldots, S^z_{i+l_1^{(B)}-1,j}, S^z_{i+l_1^{(B)},j}\}$ satisfy the property

$$S^z_{i-1,j}=S^z_{i+l_1^{(B)}+1,j}=3/2\neq S^z_{\alpha,j},$$

$$\text{for}\quad \alpha=i,i+1,i+2,\ldots,i+l_1^{(B)} \tag{21}$$

and boundary pair breaks occur between 3/2 and $S^z_{\alpha,j}\neq 3/2$. To calculate their density ρ_b we used the modified formula [see Eq. (14)]

$$\rho_b=1-\frac{1}{(L-1)L}\sum_{i=1}^{L-1}\sum_{j=1}^{L}\delta_{S^z_{i,j},3/2},\quad B>B_c. \tag{22}$$

B. The analysis of the MC results for $B\neq 0$

The MC simulations of specific heat versus magnetic-field dependences stemming from the Hamiltonian (5) taking into account the modification (17) were performed for a given set of the parameters [Eqs. (8) and (16) and $g_c=14.7, g_c'=1$] at temperatures $T_1=2.5$ K and $T_2=4.27$ K (Figs. 7 and 8). A remarkable reduction of the discrepancies between the theory and data was achieved at both temperatures. In the first case it reveals an important role of interchain correlations at a temperature T_1 quite far from the critical region while the second case indicates the significance of spin-spin correlations even at relatively high temperature T_2 where one would expect the ideal paramagnet behavior; the dashed line in Fig. 8 represents a Schottky contribution of the two lowest Kramers doublets separated by the energy $2D/k_B=20$ K split in a magnetic field $B\|z$. These rather phenomenological statements can be supported by MC calculations of the spin configurations performed at both temperatures.

In zero magnetic field the presence of mainly intrachain spin correlations is evident even at T_2 where instead of randomly distributed $S^z=\pm 3/2$ projections expected for a paramagnet one can see the clustering of chains (Fig. 9). The mean length of the ferromagnetic chain clusters $\langle l_1^{(0)}\rangle$ smoothly diminishes with the increasing temperature, qualitatively following the behavior of a correlation length of $S=1/2$ Ising ferromagnetic chain ξ,[2]

$$\xi=[\ln(\tanh(J_1/k_BT))\,]^{-1}, \tag{23}$$

with $J_1/k_B=0.85$ K; see Fig. 10. In this figure, the influence of the higher doublet on the shortening of the spin-chains was demonstrated by increasing of D from $D/k_B=10$ K up to the saturation value $D/k_B=30$ K. The comparison of the magnetic-field dependence of $\langle l_1^{(B)}\rangle$ with the corresponding theoretical predictions [the relations (6) and (7) in Ref. 4] for the 1D $S=1/2$ ferromagnetic Ising model is shown in Figs. 11(a) and 11(b). The excellent agreement between the theory

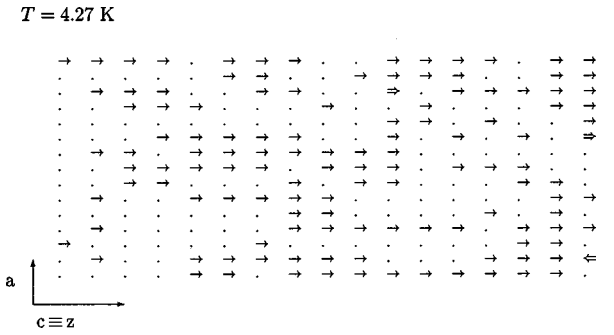

FIG. 9. The configuration segment of the snapshot created during MC run for $S=3/2$ BC model for the parameters: $L=30, T=T_2, B=0$ T, $D/k_B=10$ K. The interaction $\tilde{J}_1/k_B=0.38$ K acts in the west-east direction, whereas $\tilde{J}_2/k_B=-0.07$ K acts in the north-south direction. The symbols $\rightarrow,.,\Rightarrow,\Leftarrow$ correspond to the $S^z=3/2,-3/2,1/2,-1/2$ projections, respectively.

and data observed at both temperatures strongly indicates that the formation of two-dimensional clusters studied in the chain direction exactly resembles a behavior of the $S=1/2$ Ising chain. Further interesting observation is the fact that the quantity $\langle l_1^{(B)}\rangle$ is not sensitive to the population of a higher doublet and presence of the interchain coupling $\tilde{J}_2$ at least for the given values of parameters $\tilde{J}_1, \tilde{J}_2$ and D. However, as was shown above, both mechanisms strongly affect the thermodynamic properties. The sensitivity of the thermodynamics to the population of the higher doublet results from the energy cost necessary for the creation of $S^z=\pm 1/2$ excitations (Fig. 9).

IV. CONCLUDING REMARKS

Temperature and magnetic field dependence of $KEr(MoO_4)_2$ single-crystal specific heat was analyzed in the frame of Ising and BC models with anisotropic exchange coupling. It was found that despite of the dipolar nature of magnetic correlations in the studied system this rather phenomenological approach based on the short-range interaction

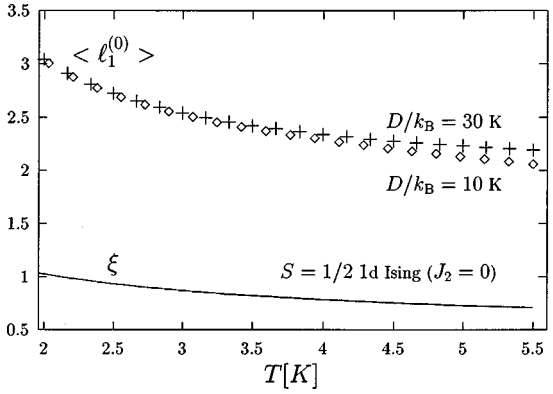

FIG. 10. Temperature dependence of the mean length $\langle l_1^{(0)}\rangle$ calculated for $S=3/2$ BC model (17) with $\tilde{J}_1/k_B=0.38$ K, $\tilde{J}_2/k_B=0.07$ K, $D/k_B=10$ K ($\diamond$), and $D/k_B=30$ K ($+$); the solid line represents a behavior of the correlation length ξ corresponding to $S=1/2$ Ising chain with $J_1/k_B=0.85$ K and $B=0$ (in units of a lattice spacing).

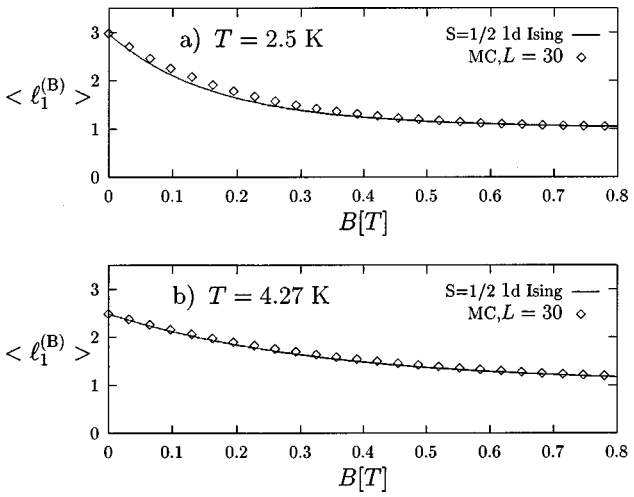

FIG. 11. (a) Magnetic field dependence of the mean length of the clusters of spins flipped in $-z$ direction, theoretically predicted for $S=1/2$ ferromagnetic Ising chain with $J_1/k_B=0.85$ K in $B\|z$ at $T_1=2.5$ K (solid line) and that calculated by MC from Eqs. (13) and (22). (b) Magnetic-field dependence of the mean length of clusters of spins flipped in $-z$ direction theoretically predicted for $S=1/2$ ferromagnetic Ising chain with $J_1/k_B=0.85$ K in $B\|z$ at $T_2=4.27$ K (solid line) and that calculated by MC from Eqs. (13) and (22).

models seems to be sufficient for the description of the KEr$(MoO_4)_2$ thermodynamics. The same observations were also found in dipolar magnets $ErBa_2Cu_3O_7$ and $ErBa_2Cu_4O_8$ where Er moments exhibit qualitatively the same ground-state magnetic structure as that predicted for KEr$(MoO_4)_2$,[22] i.e., the spins in ferromagnetic chains running in the b direction are oriented along the b axis, with adjacent chains in the ab plane coupled antiferromagnetically.[23] The results of neutron-scattering studies performed on the compounds were found to be in an excellent agreement with Onsager's exact solutions of exchange coupled $S=1/2$ Ising rectangular lattice.[23] These experimental results have triggered MC study of 2D dipolar Ising antiferromagnet with an important conclusion that for relevant range of parameters magnetic properties of the two-dimensional antiferromagnetic Ising model are not qualitatively affected by the long-range character of the dipolar interaction and the presence of dipolar interactions does not change the universality class of the system.[24] From this point of view, the current analysis of KEr$(MoO_4)_2$ suggests the system studied effectively resembles the behavior of $S=3/2$ BC model on rectangular lattice with parameters (8) and (16). Furthermore, the ground-state energy per site predicted within this model, $E_g/k_B=(\tilde{J}_1+\tilde{J}_2)/k_B=-1.01$ K, is close to $E_g/k_B=-1.32$ K, the value obtained previously from the pure dipolar approach. In future further measurements of specific heat versus magnetic-field dependence are to be performed to enable a more detailed quantitative analysis of data; the present analysis reveals that the measurements in magnetic field are not describable so excellently as the zero-field data when keeping the same parameters and it seems the analysis in field should require renormalization of the parameters. One possible explanation of the fact might result from the existence of two nonequivalent magnetic centers in the KEr$(MoO_4)_2$ unit cell.[9] To verify this assumption, further MC simulations of KEr$(MoO_4)_2$ specific heat in nonzero magnetic field are to be performed with the nonequivalence included.

A second aspect of this work is the exact validity of the Ising model for this system; the precise character of the CEF ground state suggests rather Ising-like behavior indicated by small but nonzero transversal g-factor values. It gives rise to the propagation of domain walls, thus the spin dynamics of the system might be a potential subject of future interest.

ACKNOWLEDGMENTS

We are very grateful to N. Papanicolaou for enlightening discussions on magnetic excitations. We would like to thank A. G. Anders and V. Bondarenko for clarifying discussions on the dipolar interactions and magnetic nonequivalence of Er^{3+} ions in KEr$(MoO_4)_2$. Numerical calculations of D. Blažek are gratefully acknowledged. This work was supported in part by NSF Grant No. INT-9722935 and Slovak Ministry of Education Grant Nos. 1/4385/97 and 1/6020/99.

*Electronic address: horvath@kosice.upjs.sk

[1] H.J. Mikeska and M. Steiner, Adv. Phys. **40**, 191 (1991).
[2] M. Steiner, J. Villain, and C.G. Windsor, Adv. Phys. **25**, 87 (1976).
[3] J.D. Johnson and J.C. Bonner, Phys. Rev. B **22**, 251 (1980).
[4] M. Date and M. Motokawa, Phys. Rev. Lett. **16**, 1111 (1966).
[5] A. Orendáčová, M. Orendáč, V. Bondarenko, A. Feher, and A.G. Anders, J. Phys.: Condens. Matter **10**, 1125 (1998).
[6] A.G. Anders, V.S. Bondarenko, A. Feher, A. Orendáčová, and M. Orendáč, J. Magn. Magn. Mater. **187**, 125 (1998).
[7] A.G. Anders, S.V. Volotskij, S.V. Startsev, A. Feher, and A. Orendachova, Low Temp. Phys. **21**, 38 (1995).
[8] G.I. Frolova, L.E. Reznik, and I.E. Paukov, Fiz. Tverd. Tela (Leningrad) **23**, 2160 (1981) [Sov. Phys. Solid State **23**, 1262 (1981)].
[9] A.G. Anders, S.V. Volotskij, and O.E. Zubkov, Fiz. Nizk. Temp. **20**, 131 (1994) [Low Temp. Phys. **20**, 105 (1994)].
[10] A. Anders, V. Bondarenko, A. Feher, and A. Orendacheva, Czech. J. Phys. **46**, 2093 (1996).
[11] E.N. Khatsko (private communication).
[12] J.W. Tucker, M. Saber, and L. Peliti, Physica A **206**, 497 (1994); T. Kaneyoshi, J.W. Tucker, and M. Jaščur, *ibid.* **186**, 495 (1992); T. Kaneyoshi and M. Jaščur, Phys. Rev. B **46**, 3374 (1992); M. Jaščur and T. Kaneyoshi, Phys. Status Solidi B **174**, 537 (1992).
[13] A. Lipowski and M. Suzuki, Physica A **193**, 141 (1993); T. Morita, J. Phys. Soc. Jpn. **62**, 4218 (1993).
[14] C. Domb and M.S. Green, *Phase Transitions and Critical Phenomena* (Academic Press, London, 1976), Vol. 5b; S. Wansleben and D.P. Landau, Phys. Rev. B **43**, 6006 (1990).
[15] K. Binder, *Monte Carlo Methods in Statistical Physics* (Springer, Berlin, 1979); K. Binder, *Applications of the Monte Carlo Method in Statistical Physics* (Springer, Berlin, 1984).
[16] L. Onsager, Phys. Rev. **65**, 117 (1944).
[17] M. Blume, Phys. Rev. **141**, 517 (1966).
[18] H.W. Capel, Physica (Amsterdam) **32**, 966 (1966).
[19] N. Papanicolaou and P.S. Spathis, J. Phys. C **20**, L783 (1987).
[20] M. Orendáč, A. Orendáčová, J. Černák, A. Feher, P.J.C. Signore,

M.W. Meisel, S. Merah, and M. Verdaguer, Phys. Rev. B **52**, 3435 (1995).
[21] V. Bondarenko *et al.* (unpublished).
[22] S. Simizu, S.A. Friedberg, E.A. Hayri, and M. Greenblatt, Phys. Rev. B **36**, 7129 (1987).
[23] J.W. Lynn, T.W. Clinton, W.H. Li, R.W. Erwin, J.Z. Liu, K. Vandervoort, and R. N. Shelton, Phys. Rev. Lett. **63**, 2606 (1989).
[24] A.B. MacIsaac, J.P. Whitehead, K. De'Bell, and K.S. Narayanan, Phys. Rev. B **46**, 6387 (1992).